

NNNLO results on top-quark pair production near threshold and quarkonium bound states

M. Beneke (RWTH Aachen)

8th International Symposium on Radiative Corrections (RADCOR), Firenze, October 1-5, 2007

Outline

- Motivation and status
- Theoretical framework and technical discussion
- Results related to the wave-function at the origin, $|\psi(0)|^2$
- Top-quark pair production near threshold

Work in collaboration with Y. Kiyo, K. Schuller and A.P. Penin

(Nucl.Phys.B714:67-90,2005 [hep-ph/0501289], 0705.4518 [hep-ph] (to appear in PLB), Phys.Lett.B653:53-59,2007 (0706.2733 [hep-ph]), and work in progress)

Motivation and status

- Measurement of top quark mass (target: $\delta m_t \approx 100 \text{ MeV}$) and width “Positronium” of QCD
- Basic equations:

$$(q_\mu q_\nu - q^2 g_{\mu\nu}) \Pi(q^2) = i \int d^4x e^{iq \cdot x} \langle 0 | T(j_\mu(x) j_\nu(0)) | 0 \rangle, \quad j^\mu(x) = [\bar{t} \gamma^\mu t](x)$$
$$R \equiv \frac{\sigma_{\bar{t}t}}{\sigma_0} = 12\pi e_t^2 \text{Im} \Pi(s) = \frac{18\pi e_t^2}{m_t^2} \text{Im} G_c^{(1)}(0, 0; E + i\Gamma_t)$$
$$\left(-\frac{\nabla^2(r)}{m_t} + \left[-\frac{\alpha_s C_F}{r} + 2\delta m_t \right] - E \right) G_c^{(1)}(\mathbf{r}, \mathbf{r}'; E) = \delta^{(3)}(\mathbf{r} - \mathbf{r}'), \quad E = \sqrt{s} - 2m_t$$

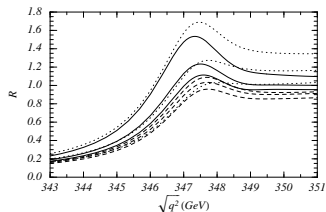
- Expansion in α_s and $v = \sqrt{\frac{\sqrt{s} - 2m_t}{m_t}}$ while $\alpha_s/v = O(1)$

$$R \sim v \sum_k \left(\frac{\alpha_s}{v} \right)^k \cdot \left\{ 1 \text{ (LO)}; \alpha_s, v \text{ (NLO)}; \alpha_s^2, \alpha_s v, v^2 \text{ (NNLO)}; \dots \right\}$$

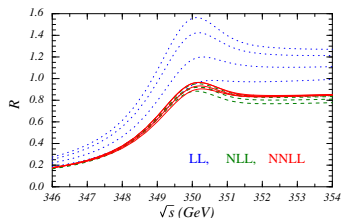
- Not discussed in this talk: appropriate top mass definitions (potential subtracted mass is used (MB,1998)), axial-vector contribution (trivial), electroweak effects (Hoang, Reiber, 2004; Kühn et al., 1990s).

Motivation and status

- NNLO calculations completed in 1998/99 find large uncertainty [up $\pm 25\%$] in the cross section in the resonance peak region (MB, Signer, Smrinov; Hoang, Teubner; Melnikov, Yelkovsky; Yakovlev; Nagano et al.; Penin, Pivovarov)
- Calculations that include a summation of logarithms of v find a much reduced scale dependence [$\pm 3\%$] (Hoang et al., 2002).
The main effect comes from the logarithms at the third order (NNNLO), not the higher order terms (Pineda, Signer, 2006).
- At NNNLO the ultrasoft scale $m_t \alpha_s^2 \sim 2 \text{ GeV}$ appears for the first time. A complete calculation of the (non-logarithmic) NNNLO correction is therefore needed.



(Beneke et al., PLB 454 (1999) 137)



(Hoang et al., PRD 65 (2002) 014014)

Feynman integrals are factorized into **hard** ($k_0 \sim k_i \sim m_t$), **soft** ($k_0 \sim k_i \sim m_t v$), **potential** ($k_0 \sim m_t v^2$, $k_i \sim m_t v$), and **ultrasoft** ($k_0 \sim k_i \sim m_t v^2$) contributions using dimensional regularization (“threshold expansion” (MB, Smirnov, 1997)).

This corresponds to the following sequence of non-relativistic effective theories (Lepage et al., 1992; Pineda, Soto, 1997; MB, 1998):

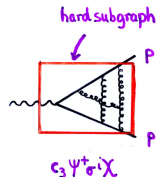
$$\begin{array}{ccc} \mathcal{L}_{\text{QCD}} [Q(h, s, p), g(h, s, p, us)] & & \mu > m \\ \downarrow & & \\ \mathcal{L}_{\text{NRQCD}} [Q(s, p), g(s, p, us)] & & mv < \mu < m \\ \downarrow & & \\ \mathcal{L}_{\text{PNRQCD}} [Q(p), g(us)] & & \mu < mv \end{array}$$

The cross section is finally obtained from a current correlation function in PNRQCD. Our new result is the complete NNNLO calculation in PNRQCD perturbation theory.

Hard matching

$$j^i = c_v \psi^\dagger \sigma^i \chi + \frac{d_v}{6m_f^2} \psi^\dagger \sigma^i \mathbf{D}^2 \chi + \dots$$

$$\mathcal{L}_{\text{QCD}} \rightarrow \mathcal{L}_{\text{NRQCD}}$$

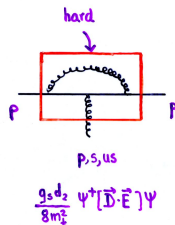


$c_v^{(2)}$ (2-loop) (MB, Signer, Smirnov; Czarnecki, Melnikov, 1997)

$c_v^{(3)}$ (3-loop) n_f -terms (Marquard et al., 2006), n_f -independent terms unknown – probably now the most important missing input

$d_v^{(1)}$ (1-loop) (Luke, Savage, 1997)

NRQCD matching (1-loop) (Manohar, 1997; Wüster, 2003)



$$\Pi(s) \rightarrow G(E) \equiv \frac{i}{2N_c(d-1)} \int d^d x e^{iEx^0} \langle 0 | T([\psi^\dagger \sigma^i \chi](x) [\chi^\dagger \sigma^i \psi](0)) | 0 \rangle$$

Soft/potential matching

Integrating out soft fluctuations results in a spatially non-local effective Lagrangian since $[k^i]_{\text{soft}} \sim [k^i]_{\text{pot}}$.

$$\begin{aligned}\mathcal{L}_{\text{PNRQCD}} = & \psi^\dagger \left(iD_0 + i\frac{\Gamma_t}{2} + \frac{\boldsymbol{\partial}^2}{2m} + \frac{\boldsymbol{\partial}^4}{8m^3} \right) \psi + \chi^\dagger \left(iD_0 - i\frac{\Gamma_t}{2} - \frac{\boldsymbol{\partial}^2}{2m} - \frac{\boldsymbol{\partial}^4}{8m^3} \right) \chi \\ & + \int d^{d-1} \mathbf{r} \left[\psi^\dagger \psi \right] (x + \mathbf{r}) \left(-\frac{\alpha_s C_F}{r} + \delta V(r, \boldsymbol{\partial}) \right) \left[\chi^\dagger \chi \right] (x) \\ & - g_s \psi^\dagger(x) \mathbf{x} \mathbf{E}(t, \mathbf{0}) \psi(x) - g_s \chi^\dagger(x) \mathbf{x} \mathbf{E}(t, \mathbf{0}) \chi(x)\end{aligned}$$

- The leading-order Coulomb potential is part of the unperturbed Lagrangian. The asymptotic states correspond to the composite field $[\psi^\dagger \chi](\mathbf{R}, \mathbf{r})$ with free propagation in the cms coordinate. **The propagation in the relative coordinate is determined by the Coulomb Green function $G_c^{(1)}(\mathbf{r}, \mathbf{r}'; E)$**
- Perturbations consist of **kinetic energy corrections**, **perturbation potentials**, and **ultrasoft gluon interactions**.
- Finite-width effects can be treated consistently only in the context of a full electroweak calculation (cf. (Hoang, Reiser, 2004) and (MB, Falgari, Kauer, Schwinn, Signer, Zanderighi, 2004/2007) for $W^+ W^-$.)

Soft/potential matching (II)

$$\delta\tilde{V} = -\frac{4\pi\alpha_s C_F}{q^2} \left[\mathcal{V}_C - \mathcal{V}_{1/m} \frac{\pi^2 |\mathbf{q}|}{m_t} + \mathcal{V}_{1/m^2} \frac{q^2}{m_t^2} + \mathcal{V}_p \frac{\mathbf{p}^2 + \mathbf{p}'^2}{2m_t^2} \right].$$

$\mathcal{V}_C^{(2)}$ (2-loop) (Schröder, 1998)

$\mathcal{V}_C^{(3)}$ (3-loop Coulomb potential) logarithmic terms (Brambilla et al., 1999; Kniehl et al. 2002), **non-logarithmic term unknown**

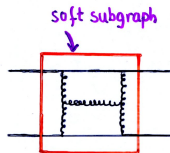
$\mathcal{V}_{1/m}^{(1)}$ (1-loop) (MB, Signer, Smirnov, 1999)

$\mathcal{V}_{1/m^2}^{(2)}$ (2-loop) (Kniehl et al., 2001), $\mathcal{O}(\epsilon)$ term unknown

$\mathcal{V}_{1/m^2}, \mathcal{V}_p$ (1-loop) (Kniehl et al., 2002; Wüster, 2003), $\mathcal{O}(\epsilon)$ should be checked.

See 0705.4518 [hep-ph] for explicit d -dimensional expressions

The unknown potential coefficients are probably numerically not important.

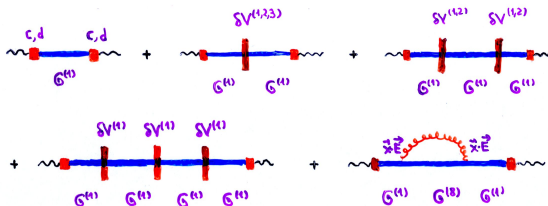


$$\int d^3\vec{r} [\psi^\dagger \psi](\vec{r}) \int \frac{d^{d-1}\vec{q}}{(2\pi)^{d-1}} e^{i\vec{q}\cdot\vec{r}} \frac{b_2(\epsilon)}{m_t |\vec{q}|} [\chi^\dagger \chi](0)$$

NNNLO calculation

The NNNLO contribution to the PNRQCD correlation function is

$$G^{(3)} = -G_c^{(1)} \delta V_1 G_c^{(1)} \delta V_1 G_c^{(1)} \delta V_1 G_c^{(1)} + 2G_c^{(1)} \delta V_1 G_c^{(1)} \delta V_2 G_c^{(1)} - G_c^{(1)} \delta V_3 G_c^{(1)} + \delta G_{\text{us}}$$



where

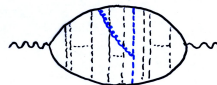
$$G_c^{(1,8)}(\mathbf{r}, \mathbf{r}', E) = \frac{m\mathbf{y}}{2\pi} e^{-y(r+r')} \sum_{l=0}^{\infty} (2l+1)(2\mathbf{y}\mathbf{r})^l (2\mathbf{y}\mathbf{r}')^l P_l \left(\frac{\mathbf{r} \cdot \mathbf{r}'}{rr'} \right) \sum_{s=0}^{\infty} \frac{s! L_s^{(2l+1)}(2\mathbf{y}\mathbf{r}) L_s^{(2l+1)}(2\mathbf{y}\mathbf{r}')}{(s+2l+1)!(s+l+1-\lambda)}$$

$$y = \sqrt{-m(E+i\epsilon)}, \quad \lambda = \frac{m\alpha_s}{2y} \times \{C_F \text{ (singlet); } C_F - C_A/2 \text{ (octet)}\}$$

For singlet need only $l = 0$, for octet only $l = 1$.

NNNLO calculation (II)

The ultrasoft contribution is ($D = d - 1$)



$$\delta G_{\text{us}} = (-i)(ig_s)^2 C_F \int \frac{d^d k}{(2\pi)^d} \frac{-i}{k^2} \left(\frac{k^i k^j}{k_0^2} - \delta^{ij} \right) \int \prod_{n=1}^6 \frac{d^D p_n}{(2\pi)^D} i\tilde{G}^{(1)}(p_1, p_2; E) i\tilde{G}^{(8)}(p_3, p_4; E + k^0) i\tilde{G}^{(1)}(p_5, p_6; E) \\ \times i \left[\frac{2p_3^i}{m_t} (2\pi)^D \delta^{(D)}(p_3 - p_2) + (ig_s)^2 \frac{C_A}{2} \frac{2(p_2 - p_3)^i}{(p_2 - p_3)^4} \right] i \left[-\frac{2p_4^j}{m_t} (2\pi)^D \delta^{(D)}(p_4 - p_5) + (ig_s)^2 \frac{C_A}{2} \frac{2(p_4 - p_5)^j}{(p_4 - p_5)^4} \right]$$

- In position space only three instead of seven integrations, but the integrals are divergent and the $1/\epsilon$ poles must be extracted in momentum space.
- The Coulomb Green functions are not known in D dimensions.
- UV divergence in the ultrasoft k integral is related to potentials and the derivative current. UV divergence in potential p_i integrals are related to the non-relativistic vector current.
- **Strategy: identify divergent subgraphs, calculate them in D dim. momentum space, combine with counterterm and perform remaining integrations in three dimensions.**

NNLO calculation (III)

Example of divergence extraction:

$$\begin{aligned}
 [G_{nC}^{(3)}]_{div} &= \left[-\frac{1}{\epsilon^2} \left(\frac{7}{12} C_F^2 + \frac{2}{9} C_A^2 + \frac{23}{48} C_A C_F + \beta_0 \left(\frac{C_A}{24} + \frac{C_F}{36} \right) \right) \right. \\
 &\quad - \frac{1}{\epsilon} \left\{ \left(\frac{11}{24} - \frac{L_m}{12} \right) C_F^2 + \left(\frac{427}{324} - \frac{4 \ln 2}{3} - \frac{L_m}{8} \right) C_A C_F - \left(\frac{5}{216} + \frac{2 \ln 2}{3} \right) C_A^2 \right. \\
 &\quad \left. \left. + \left(\frac{C_A}{24} + \frac{C_F}{54} \right) \beta_0 - \left(\frac{1}{30} - \frac{29 n_f}{162} \right) C_F T_F + \frac{49}{216} C_A T_F n_f \right\} \right] \frac{\alpha_s^3 C_F}{\pi} \langle 0 | \hat{G}_c^{(1)} | 0 \rangle \\
 &\quad - \left[\frac{1}{4} C_A + \frac{1}{6} C_F \right] \frac{\alpha_s^2 C_F}{\epsilon} \langle 0 | \hat{G}_c^{(1)} \delta V_1 \hat{G}_c^{(1)} | 0 \rangle \quad (L_m = \ln(\mu/m))
 \end{aligned}$$

The ultrasoft contribution is more complicated. Extract the vertex divergence by subtracting three-loop vertex diagrams at zero momentum:



The remaining finite parts are expressed as (multiple) sums of Gamma functions, PolyGamma functions, Hypergeometric functions in case of potential corrections and numerical integrations in case of the ultrasoft correction. Pole parts are cancelled analytically.

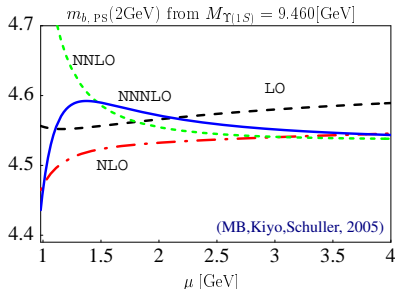
$\Upsilon(nS)$ results

The correlation function has bound state poles. Their location provides the quarkonium masses, their residue the leptonic decay width.

$$\Pi(q^2) \stackrel{E \rightarrow E_n}{=} \frac{N_c}{2m^2} \frac{Z_n}{E_n - E - i\epsilon}.$$

$$M_{\Upsilon(nS)} = 2m_b + E_n$$

$$\Gamma(\Upsilon(nS) \rightarrow l^+ l^-) = \frac{4\pi N_c e^2 \alpha^2 Z_n}{3m_b^2}$$



Determine the PS mass from the $\Upsilon(1S)$ mass.

$$m_{b,ps}(2\text{ GeV}) = (4.57 \pm 0.03_{\text{pert.}} \pm 0.01_{\alpha_s} \pm 0.07_{\text{non-pert.}}) \text{ GeV}$$

$$\implies \overline{\text{MS}} \text{ mass: } m_b(m_b) = (4.23 \pm 0.08) \text{ GeV}$$

Perturbation theory does not converge for the excited states $n > 1$.

$\Upsilon(nS)$ results (II)

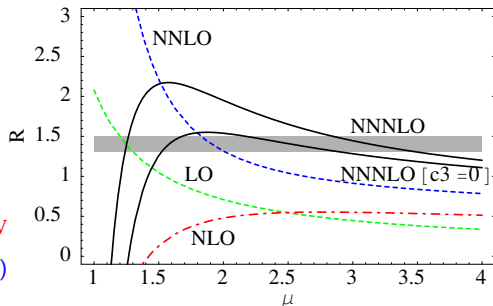
$$\Gamma(\Upsilon(nS) \rightarrow l^+l^-) = \frac{4\pi N_c e^2 Q^2 \alpha^2 Z_n}{3m_b^2}$$

$$Z_n = \frac{(m_b \alpha_s(\mu_0) C_F)^3}{8\pi n^3} \times R_n$$

$$R_n = \left(\frac{\alpha_s(\mu)}{\alpha_s(\mu_0)} \right)^3 \times (1 + \dots)$$

$$\Gamma(\Upsilon(1S) \rightarrow l^+l^-)_{\text{exp}} = (1.340 \pm 0.018) \text{ keV}$$

$$\Rightarrow [R_1]_{\text{exp}} = (1.4 \pm 0.1) \quad (\mu_0 = 2 \text{ GeV})$$



- Reduction of scale-dependence (if c_3 is small).
- Result consistent with experimental value within large remaining uncertainty (note: NNLL result was too small)
- Non-perturbative effects?

Here and in the following the NNNLO result is shown for two values of c_3 : 1) including the known n_f -dependent terms; 2) setting c_3 to zero. The Log μ terms, which are known completely, are **always** included.

“Toponium” residue

There are no toponium bound states, but Z_1 is roughly related to the height of the cross section peak:

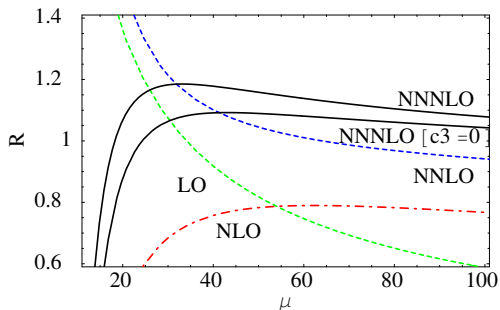
$$R_{\text{peak}} \approx 6\pi N_c e_t^2 Z_1 / (m_t^2 \Gamma_t)$$

$$\begin{aligned} Z_1 &= \frac{(m_b \alpha_s C_F)^3}{8\pi} \times \left(1 + \alpha_s \left[-2.13 + 3.66 L \right] \right. \\ &\quad \left. + \alpha_s^2 \left[8.38 - 7.26 \ln \alpha_s - 13.40 L + 8.93 L^2 \right] \right. \\ &\quad \left. + \alpha_s^3 \left[11.01 + [37.58]_{c_3, n_f} - 9.79 \ln \alpha_s - 16.35 \ln^2 \alpha_s \right. \right. \\ &\quad \left. \left. + (53.17 - 44.27 \ln \alpha_s) L - 48.18 L^2 + 18.17 L^3 \right] \right) \quad \left(L = \ln \frac{\mu}{m_t C_F \alpha_s} \right) \\ &= \frac{(m_b \alpha_s C_F)^3}{8\pi} \times \left(1 - 2.13 \alpha_s + 22.64 \alpha_s^2 + [-32.96 + [37.58]_{c_3, n_f}] \alpha_s^3 \right) \\ &\quad \text{(for } \alpha_s = 0.14, L = 0 \text{)} \end{aligned}$$

- Typical size of non-logarithmic terms of individual third-order corrections (ultrasoft, non-Coulomb potentials, Wilson coefficient) is about $40\alpha_s^3 \approx 10\%$ (more than 100% for bottomonium!)
- Cancellations between individual terms and between logarithmic and non-logarithmic terms occur.

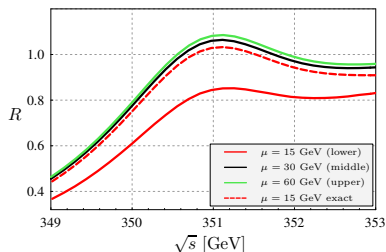
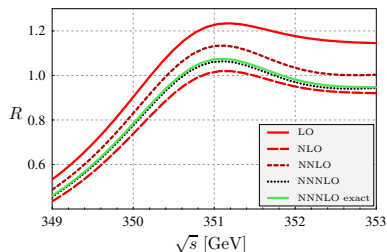
“Toponium” residue (II)

Plot shows $R \equiv Z_1/Z_1^{\text{LO}}(\mu_0 = 30 \text{ GeV})$



- Strong reduction of scale-dependence
- Result unstable for $\mu < 20 \text{ GeV}$. Should one be concerned about this?

$t\bar{t}$ cross section - Coulomb correction

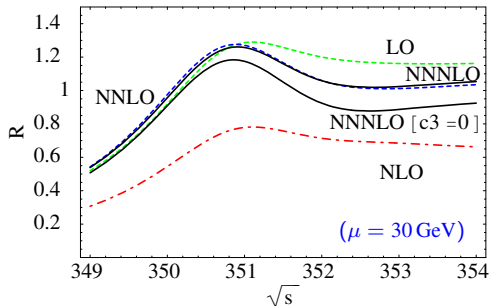


Normalized top pair production cross section (Coulomb corrections only) for $m_{t,ps} = 175$ GeV, $\Gamma_t = 1.5$ GeV. Left figure: successive approximations up to the third order ($\mu = 30$ GeV). Right figure: scale dependence at third order. (MB, Kiyo, Schuller; 2005)

With only the Coulomb potential included, multiple insertions can be resummed into the propagator (Coulomb Green function) using the numerical solution of the Schrödinger equation (Peskin, Strassler, 1991). The right plot shows that the large scale dependence at $\mu < 20$ GeV is an artefact of perturbation theory. The exact solution is stable \implies don't consider $\mu < 25$ GeV.

NNNLO $t\bar{t}$ cross section

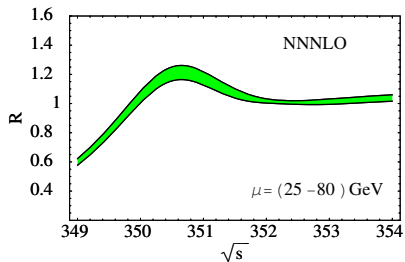
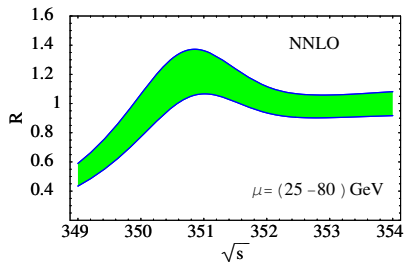
The following results use: $m_{t,PS}(20\text{ GeV}) = 175\text{ GeV}$, $\Gamma_t = 1.4\text{ GeV}$, $\alpha_s(M_Z) = 0.1189$.
Results are unpublished \equiv preliminary!



Size of the third-order correction (probably) up to 10% (at this scale).
Convergence!

NNNLO $t\bar{t}$ cross section (II)

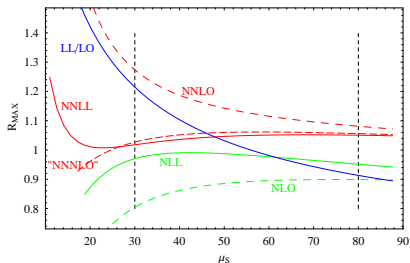
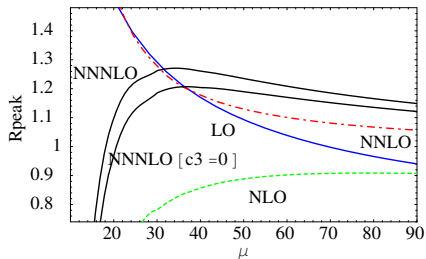
Scale dependence at NNNLO versus NNLO.



(NNNLO includes all known c_3 terms.)

NNNLO $t\bar{t}$ cross section (III)

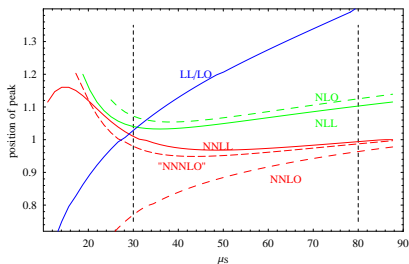
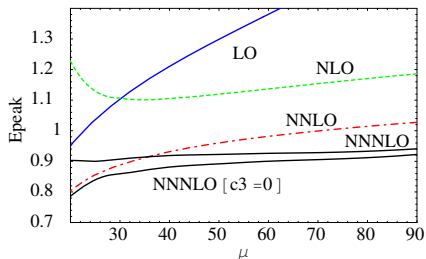
Comparison of the cross section maximum in the fixed-order and renormalization group approach (right plot from (Pineda, Signer, 2006))



- The cross section maximum is about 15% higher than in the renormalization-group approach due to the large positive non-logarithmic term.
- Residual scale dependence similar in both approaches. The renormalization group captures correctly the logarithms of μ .

NNNLO $t\bar{t}$ cross section (IV)

Comparison of the position of the cross section maximum in the fixed-order and renormalization group approach (right plot from (Pineda, Signer, 2006)). $E_{\text{peak}} \equiv \sqrt{s} - 2m_{t,\text{PS}}$.



- The peak position shift by about 100 MeV relative to the NNLL renormalization group improved result and its scale-dependence is significantly below 100 MeV. PS mass scheme is essential.
- Probably meets foreseen experimental accuracy on m_t .
- Need four-loop (formally even five-loop) relation between the pole and the MSbar mass to convert the precise value for the PS mass to an equally precise value of the MSbar mass.

- Third-order QCD correction to the $t\bar{t}$ cross section near threshold is nearly complete. A few matching coefficients are missing, of which the n_f -independent term of the third-order matching of the vector current to NRQCD is probably the most important.
- Conclusions:
 - After the huge NNLO correction the third-order correction behaves well and removes a large part of the theoretical uncertainty.
 - Non-logarithmic terms are important and increase the cross section relative to the (partial) NNLL result by about 15% (unless c_3 is ...)
- Further work should be done on electroweak and finite-width effects.